

## SPIN-POLARONS IN AN EXCHANGE MODEL

O. NAVARRO\*, E. VALLEJO<sup>†</sup> and M. AVIGNON<sup>‡</sup>

*\*Instituto de Investigaciones en Materiales, Universidad Nacional Autónoma de México,  
Apartado Postal 70-360, 04510 México D. F., México*

*†Facultad de Ingeniería Mecánica y Eléctrica, Universidad Autónoma de Coahuila,  
Carretera Torreón-Matamoros Km. 7.5 Ciudad  
Universitaria C.P. 27276 Torreón, Coahuila, Mexico*

*‡Institut Néel, CNRS and Université Joseph Fourier,  
Boite Postale 166, 38042 Grenoble, France  
†emapion@yahoo.com*

Received 14 November 2011

Published 3 April 2012

Spin-polarons are obtained using an Ising-like exchange model consisting of double and super-exchange interactions in low-dimensional systems. At zero temperature, a new phase separation between small magnetic polarons, one conduction electron self-trapped in a magnetic domain of two or three sites, and the antiferromagnetic phase was previously reported. On the other hand the important effect of temperature was missed. Temperature diminishes Boltzmann probability allowing excited states in the system. Static magnetic susceptibility and short-range spin-spin correlations at zero magnetic field were calculated to explore the spin-polaron formation. At high temperature Curie-Weiss behavior is obtained and compared with the Curie-like behavior observed in the nickelate one-dimensional compound  $Y_{2-n}Ca_nBaNiO_5$ .

*Keywords:* Exchange and super-exchange interactions; classical spin models; phase separation.

PACS numbers: 75.30.Et, 75.10.Hk, 64.75.+g

### 1. Introduction

Phase transition in a given physico-chemical system is characterized by parameters like the range of the microscopic interactions, the space dimensionality  $d$  and the dimensionality of the order parameter, often referred to the spin dimensionality  $s$ . There are features whose qualitative nature is determined by the universality class to which the system belongs. Short-range interactions, double and super-exchange nearest-neighbor type, classical and quantum spins  $s$  in  $d$ -dimensional systems have been studied.<sup>1-17</sup> Double-exchange (DE) interaction or indirect exchange, is the source of a variety of magnetic behavior in transition metal and rare-earth compounds.<sup>18</sup> The origin of DE lies in the intra-atomic coupling of the spin of itinerant

electrons with localized spins  $\mathbf{S}_i$ . This coupling favors a ferromagnetic (F) background of local spins and may lead to interesting transport properties such as colossal magnetoresistance. This mechanism has been widely used in the context of manganites.<sup>1-3,19,20</sup> This F tendency is expected to be frustrated by antiferromagnetic (AF) inter-atomic super-exchange (SE) interactions between localized spins  $\mathbf{S}_i$  as first discussed by de Gennes<sup>4</sup> who conjectured the existence of canted states. In spite of recent interesting advances, our knowledge of magnetic ordering resulting from this competition is still incomplete.

Although it may look academic, the one-dimensional (1D) version of this model is very illustrative and helpful in building an unifying picture. On the other hand, the number of pertinent real 1D systems as the nickelate one-dimensional metal oxide carrier-doped compound  $Y_{2-n}Ca_nBaNiO_5$ <sup>21,22</sup> is increasing. Haldane gap ( $\sim 9$  meV) has been observed for the parental compound  $n = 0$   $Ni^{2+}$  ( $S = 1$ ) from susceptibility and neutron scattering measurements. In these compounds, carriers are essentially constrained to move parallel to NiO chains and a spin-glass-like behavior was found at very low temperature  $T \lesssim 3$  K for typical dopings  $n \approx 0.04, 0.1$  and  $0.15$ . At high temperature Curie-like behavior of the magnetic susceptibility was found. The question is how physical properties change by introducing  $n$  holes in the system. In the doped case the itineracy of doped electrons or holes plays an important role taken into account by the DE mechanism. Recently, it has been shown that three-leg ladders in the oxyborate system  $Fe_3BO_5$  may provide evidence for the existence of spin and charge ordering resulting from such a competition.<sup>23</sup>

Naturally, the strength of the magnetic interactions depends significantly on the conduction electron band filling,  $x = 1 - n$ . At low conduction electron density, F polarons have been found for localized  $S = 1/2$  quantum spins.<sup>9,10</sup> "Island" phases, periodic arrangement of F polarons coupled antiferromagnetically, have been clearly identified at commensurate fillings both for quantum spins in one dimension<sup>12,13</sup> and for classical spins in one<sup>11</sup> and two dimensions.<sup>14</sup> Phase separation between hole-undoped antiferromagnetic and hole-rich ferromagnetic domains has been obtained in the Ferromagnetic Kondo model.<sup>5,6</sup> Phase separation and small ferromagnetic polarons have been also identified for localized  $S = 3/2$  quantum spins.<sup>15</sup> In addition to the expected F-AF phase separation appearing for small SE coupling, a new phase separation between small polarons ordered (one electron within two or three sites) and AF regions for larger SE coupling was found.<sup>16,17</sup> These phase separations are degenerate with phases where the polarons can be ordered or not giving a natural response to the instability at the Fermi energy and to an infinite compressibility as well. Wigner crystallization and spin-glass-like behavior were also obtained and could explain the spin-glass-like behavior observed in the nickelate 1D doped compound  $Y_{2-n}Ca_nBaNiO_5$ .<sup>16</sup>

In this paper, we present a study of the parallel static magnetic susceptibility in an Ising-like exchange model. Short-range spin-spin correlations are also presented.

Our results are compared with the Curie-like behavior observed at high temperature in the nickelate one-dimensional compound  $\text{Y}_{2-n}\text{Ca}_n\text{BaNiO}_5$ .<sup>21,22</sup> The paper is organized as follows. In Sec. 2 a brief description of the model is given. In Sec. 3, results and a discussion are presented. Finally, our results are summarized in Sec. 4.

## 2. The Model

The DE Hamiltonian is originally of the form,

$$H = - \sum_{i,j;\sigma} t_{ij} (c_{i\sigma}^+ c_{j\sigma} + \text{h.c.}) - J_H \sum_i \mathbf{S}_i \cdot \boldsymbol{\sigma}_i, \quad (1)$$

where  $c_{i\sigma}^+$  ( $c_{i\sigma}$ ) are the fermions creation (annihilation) operators of the conduction electrons at site  $i$ ,  $t_{ij}$  is the hopping parameter and  $\boldsymbol{\sigma}_i$  is the electronic conduction band spin operator. In the second term,  $J_H$  is the Hund's exchange coupling. Here, Hund's exchange coupling is an intra-atomic exchange coupling between the spins of conduction electrons  $\boldsymbol{\sigma}_i$  and the spin of localized electrons  $\mathbf{S}_i$ . This Hamiltonian simplifies in the strong coupling limit  $J_H \rightarrow \infty$ , a limit commonly called itself the DE model. In this strong coupling limit itinerant electrons are now either parallel or anti-parallel to local spins and are thus spinless. The complete one-dimensional DE+SE Hamiltonian becomes,

$$H = -t \sum_i \left( \cos \left( \frac{\phi_{i,i+1}}{2} \right) c_i^+ c_{i+1} + \text{h.c.} \right) + J \sum_i \mathbf{S}_i \cdot \mathbf{S}_{i+1}, \quad (2)$$

$\phi_{i,i+1}$  is the relative angle between localized spins at sites  $i$ ,  $i+1$  defined with respect to a  $z$ -axis taken as the spin quantization axis of the itinerant electrons. The SE coupling is an antiferromagnetic inter-atomic exchange coupling between localized spins  $\mathbf{S}_i$ . This coupling is given in the second term of the former equation. Here  $J$  is the SE interaction energy. An Ising-like model with itinerant electrons will be considered in this paper, i.e.,  $d = 1$ ;  $s = 1$  and  $\phi_i = 0$  or  $\pi$ . For itinerant electrons (holes) an electron (hole)-single approximation will be used. The nickelate one-dimensional parental compound  $\text{Y}_2\text{BaNiO}_5$ , is basically formed of quasi one-dimensional chains of  $\text{Ni}^{2+}$ .  $3d_{3z^2-r^2}$  and  $3d_{x^2-y^2}$  are two relevant  $\text{Ni}^{2+}$  orbitals in this system.  $3d_{x^2-y^2}$  is basically localized while  $3d_{3z^2-r^2}$  has finite overlap with  $2p_z$  orbital of the O.<sup>24,25</sup> So, to make contact with the nickelate one-dimensional compound  $\text{Y}_{2-n}\text{Ca}_n\text{BaNiO}_5$ ,  $N$  localized  $S = 1/2$  spins in the  $3d_{x^2-y^2}$  orbital will be considered. On the other hand itinerant electrons  $x$  or holes  $n$  will be placed in the  $3d_{3z^2-r^2}$  orbital. The role of these electrons (holes) within the parental compound  $n = 0$ , will be considered by the DE mechanism. Within our Ising-like model there is an electron-hole symmetry.

Exact parallel static magnetic susceptibility  $\chi$  and short-range spin-spin correlations are presented using a standard canonical ensemble. To obtain  $\chi$  within

the electron (hole)-single approximation is necessary to calculate eigenvalues of the following matrix

$$\mathbf{H} = \begin{pmatrix} h_1 & t_{1,2} & 0 & 0 & \cdots \\ t_{2,1} & h_2 & t_{2,3} & 0 & \cdots \\ 0 & t_{3,2} & h_3 & t_{3,4} & \cdots \\ 0 & 0 & t_{4,3} & h_4 & \cdots \\ \vdots & \vdots & \vdots & \vdots & \ddots \end{pmatrix} \quad (3)$$

where

$$h_i = JS^2 \sum_{k=1}^{N-1} \cos(\phi_k - \phi_{k+1}) - \mu B \sum_{k=1}^N \cos(\phi_k) - \mu B \cos(\phi_i), \quad (4)$$

in the former equation first term is SE interaction and the second one is the Zeeman coupling of the localized background of  $S = 1/2$  spins. Third term is the coupling between the magnetic moment  $\mu$  of the itinerant electron and the magnetic field  $B$ . A magnetic field was introduced to calculate  $\chi$ .

$$t_{i,j} = t_{j,i} = -t \cos((\phi_k - \phi_{k+1})/2). \quad (5)$$

With eigenvalues of Eq. (3), it is easy to obtain partition function  $Z$  in the canonical ensemble within the electron-single approximation

$$Z = \sum_{i < j < k, \dots} e^{-\beta(\epsilon_i + \epsilon_j + \epsilon_k + \dots)}. \quad (6)$$

For one ( $i$ ), two ( $i$  and  $j$ ), three ( $i$ ,  $j$  and  $k$ ) and ( $\dots$ ) itinerant electrons, respectively.  $\beta = \frac{1}{k_B T}$  being  $k_B$  Boltzmann constant and  $T$  temperature.

Magnetic susceptibility is related with partition function as

$$\chi = \lim_{B \rightarrow 0} k_B T \frac{\partial^2}{\partial B^2} \ln Z. \quad (7)$$

Mean value of all operators can be related to partition function i.e.,  $\langle A \rangle$

$$\langle A \rangle = \frac{\sum_{i < j < k, \dots} A e^{-\beta(\epsilon_i + \epsilon_j + \epsilon_k + \dots)}}{Z}. \quad (8)$$

On the other hand, the phenomenological Ising-like model was proposed because of our previous results using classical localized spins lead basically to an Ising-like model.<sup>16,17</sup> High temperature  $\chi$  will be compared with experimental results of the nickelate one-dimensional compound  $Y_{2-n}Ca_nBaNiO_5$ .<sup>21,22</sup>

### 3. Results and Discussion

In this section, phase diagram, parallel static magnetic susceptibility MS and short-range spin-spin correlations are presented for a particular open linear chain of  $N = 20$  sites. In the thermodynamic limit, phase diagram is shown in Fig. 1.

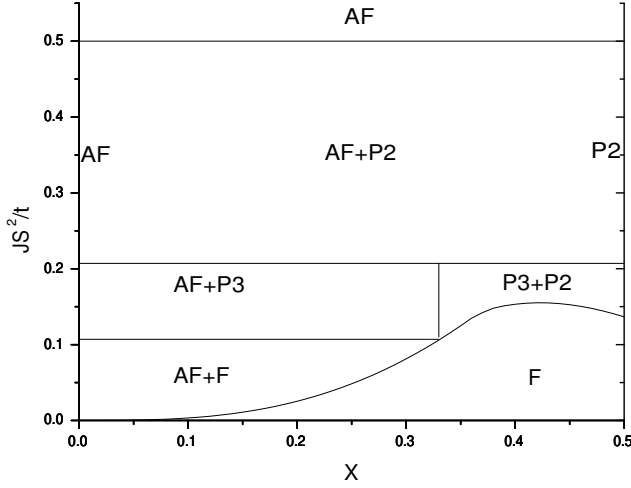


Fig. 1. Itinerant electron density  $x$  versus SE interaction energy  $JS^2/t$  phase diagram.

This phase diagram is similar to our previous one using classical localized spins ( $s = 3$ ).<sup>16,17</sup> Phase separation between ferromagnetic (F)  $\cdots \uparrow\uparrow\uparrow\uparrow\uparrow \cdots$  and antiferromagnetic (AF)  $\cdots \uparrow\downarrow\uparrow\downarrow \cdots$  phases is found for low SE interaction energy. On the other hand phase separation between P2  $\cdots \uparrow\uparrow\downarrow\uparrow\uparrow \cdots$  and P3  $\cdots \uparrow\uparrow\uparrow\downarrow\downarrow\uparrow\uparrow \cdots$  phases and the AF phase was obtained for high  $JS^2/t$ . Because of the scalar  $s = 1$  spin character used in this paper canted CP3, CP2 and T phases are not obtained in this paper.<sup>16,17</sup> The AF phase observed at  $x = 0$  was previously studied for an Ising ( $s = 1$ ) and classical ( $s = 3$ ) model respectively in Refs. 26 and 27.

Figures 2–4 show the inverse of the magnetic susceptibility versus temperature for one, two and three itinerant electrons, respectively. Solid lines in those figures represent high temperature  $J_H \gg k_B T \gg t \gg JS^2$  limit. Curie–Weiss behavior can be easily observed in those figures as  $(\chi t / N \mu^2) = C / (k_B T / t + k_B T_c / t)$ ; being  $C$  Curie constant and  $T_c$  Curie–Weiss-like temperature. ( $C = 1.15$ ;  $(k_B T_c / t) = 0.35$ ), ( $C = 1.30$ ;  $(k_B T_c / t) = 0.31$ ) and ( $C = 1.44$ ;  $(k_B T_c / t) = 0.28$ ) for one, two and three itinerant electrons, respectively. Curie constant can be rigorously extracted for the former limit  $J_H \rightarrow \infty$  and  $t = J = 0$ . For this goal it is considered  $N$  localized spins and  $N_e$  itinerant electrons. Because of  $J_H \rightarrow \infty$  limit Hilbert space is reduced. So there are  $N_e$  and  $N - N_e$  free particles with  $\pm 2\mu B$  and  $\pm \mu B$  energies, respectively, where  $B$  is the magnetic field. The former gives  $\chi t / N \mu^2 = (1 + 3x) / (k_B T / t)$ . Curie constant is identified like  $1 + 3x$ . It gives 1.15, 1.30 and 1.45 for one, two and three itinerant electrons, respectively, i.e., ( $x = 0.05, 0.10$  and  $0.15$ ). These values are very close to those obtained in Figs. 2–4. Now, we can use our Curie constant  $1 + 3x$  to make contact with results of the nickelate one-dimensional compound  $Y_{2-n}Ca_nBaNiO_5$ .  $3n$  ( $S = 1/2$ ) for Curie constant was proposed by Kojima *et al.*<sup>21,22</sup> Kojima *et al.* proposed that each Ca-atom introduces three  $S = 1/2$  spins.

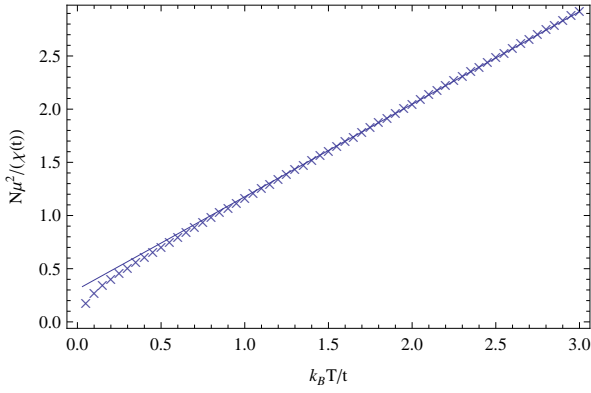


Fig. 2. Inverse of the magnetic susceptibility ( $\chi$ ) versus temperature ( $k_B T/t$ ) for  $x = 0.05$  i.e., one itinerant electron and a typical value of the SE interaction energy  $JS^2/t = 0.2$ . Curie-Weiss-like behavior at high temperature limit can be observed. Solid line represents  $J_H \gg k_B T \gg t \gg JS^2$  limit.

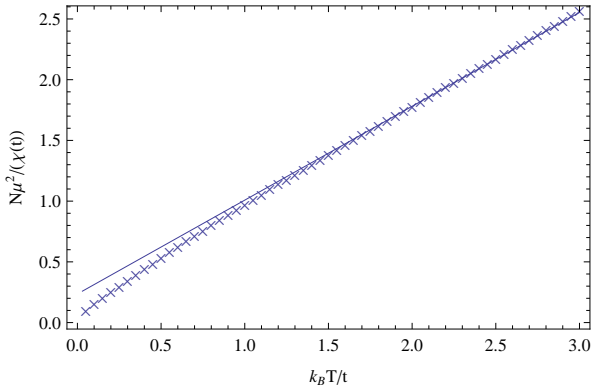


Fig. 3. The same as Fig. 2 but for two itinerant electrons  $x = 0.10$ .

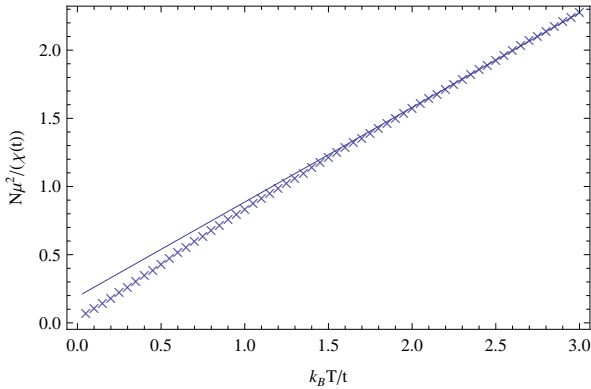


Fig. 4. The same as Fig. 2 but for three itinerant electrons  $x = 0.15$ .

They studied hole dopings  $n = 0.045, 0.095$  and  $0.149$ . In our case these itinerant holes correspond to  $x = 0.955, 0.905$  and  $0.851$  itinerant electrons studied here. It means Curie constant  $(1 + 3x)$  as  $C = 3.865, 3.715$  and  $3.553$  or simply  $C = 4 - 3n$  if we introduce holes as Kojima.  $n = 0$  corresponds to  $C = 4$  or  $N_e = N$  electrons coupled with  $N$  localized spins  $S = 1/2$  by an infinite Hund's coupling. On the other hand,  $n = 1$  is exactly  $N$  localized spins  $S = 1/2$  with  $C = 1$ . So, the effect to introduce holes in our itinerant electron system is to reduce Curie constant. For low temperature the model proposed by Kojima *et al.* is very close to our P3+AF phase separation. On the other hand, Curie-Weiss-like temperature  $T_c$  decreases as itinerant electron density increases. Itinerant electrons are responsible for the former F behavior because of our DE interaction.

Short range spin-spin correlations  $\langle S_i S_{i+1} / S^2 \rangle$  at zero magnetic field can be observed in Figs. 5–7 for a typical value of  $JS^2/t = 0.2$  and four different temperatures  $k_B T/t = 0.01, 0.1, 1.0, 10$ , solid circles, cross, large open circles and plus symbols, respectively, were used. To obtain these short range correlations negative in-site ( $\epsilon/t = -0.1$ ) energies were used to pin one, two and three polarons in the linear chain as can be observed in Figs. 5–7, respectively. These negative in-site energies can be related with impurities in our linear chain. For low temperature polarons of three sites in an AF background can be clearly seen. Similar polarons were found in Ref. 15 by using quantum  $S = 3/2$  core spins. This phase with disordered polarons is degenerated to our P3+AF phase separation. It means ordered polarons of three sites in an AF background. At high temperature ( $(k_B T/t) > 0.1$ ) polarons disperse and a very low correlation is observed.

In the same way, Figs. 8–10 show short range spin-spin correlations  $\langle S_i S_{i+1} / S^2 \rangle$  for another typical value of  $JS^2/t = 0.02$  and three different temperatures  $k_B T/t = 0.01, 0.1$  and  $1.0$ . In this case only one in-site ( $\epsilon/t = -0.1$ ) energy was utilized to pin the F phase as can be seen in Figs. 8–10. For low temperature F–AF phase separation can be observed. The F phase increases as the itinerant electron density  $x$  increases, see Figs. 8–10. The former is because of DE interaction. At high temperature the F phase disperses and a very low correlation is observed.

It is tempting to apply our results to the magnetic properties of the hole doped  $Y_{2-n}Ca_nBaNiO_5$ . Doing so raises the question of the relation between quantum spins and classical spins cases. It is clear that some properties are specific to the quantum character of the spins, in particular the Haldane gap occurring in Heisenberg  $S = 1$  chains, as in the case of undoped  $Y_2BaNiO_5$ . However, in the doped case the itinerancy of doped electrons or holes plays an important role taken into account by the DE mechanism. The essential behavior of the spin correlations in the quantum level is similar in the classical case. For the commensurate filling  $x = 1/2$  the polaronic phase P2 in Ref. 16 is qualitatively similar to the quantum  $S = 1/2$  case.

We have calculated magnetic susceptibility for typical values of the conduction electron density to make contact with experiments.<sup>21,22</sup> The inverse of magnetic susceptibility ( $\chi$ ) versus  $T$  presents a complicated behavior as described in the

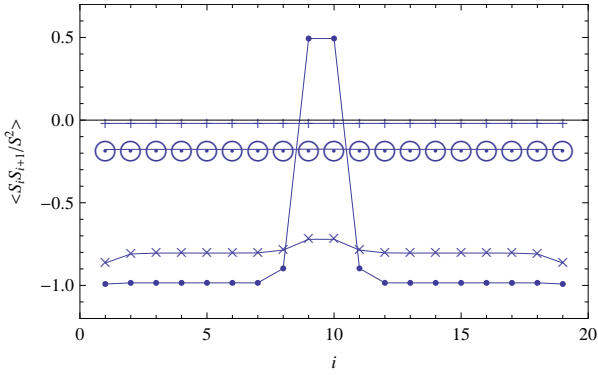


Fig. 5. Short-range spin-spin correlations within our Ising-like model for one itinerant electron  $x = 0.05$  and  $JS^2/t = 0.2$ . Solid circles, cross, large open circles and plus symbols represent four different temperatures  $k_B T/t = 0.01, 0.1, 1.0$  and  $10$ , respectively.

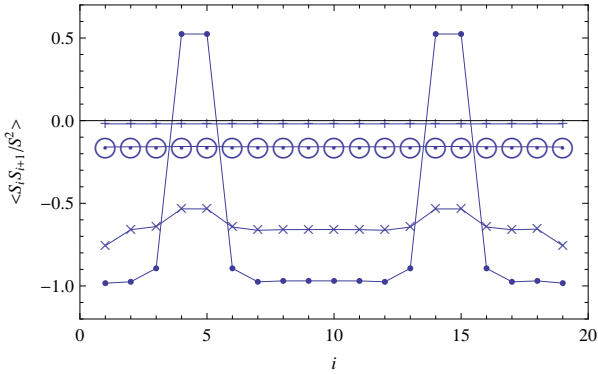


Fig. 6. The same as Fig. 5 but for two itinerant electrons  $x = 0.10$ .

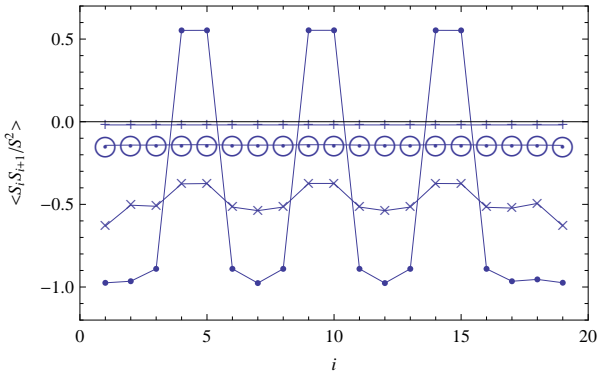


Fig. 7. The same as Fig. 5 but for three itinerant electrons  $x = 0.15$ .



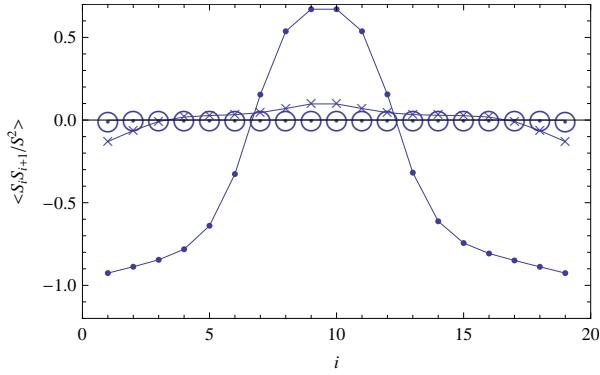


Fig. 8. Short-range spin-spin correlations for one itinerant electron  $x = 0.05$  and  $JS^2/t = 0.02$ . Solid circles, cross and large open circles represent three different temperatures  $k_B T/t = 0.01, 0.1$  and  $1.0$ , respectively.

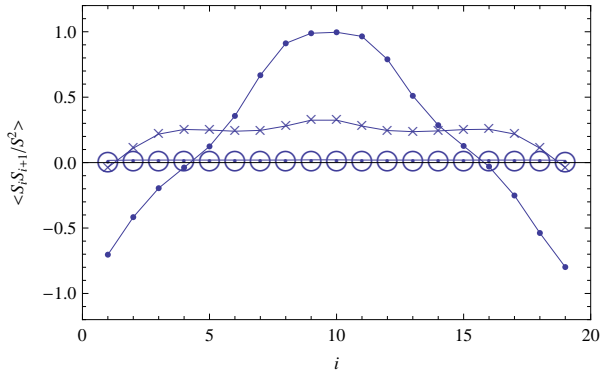


Fig. 9. The same as Fig. 8 but for two itinerant electrons  $x = 0.10$ .

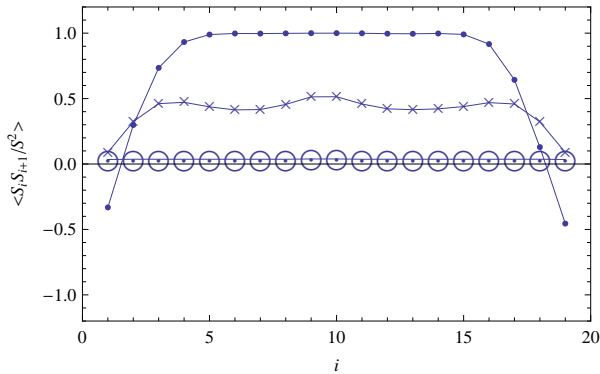


Fig. 10. The same as Fig. 8 but for three itinerant electrons  $x = 0.15$ .

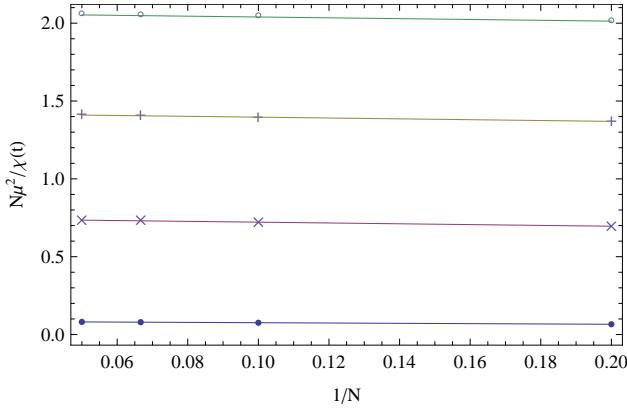


Fig. 11. Inverse of magnetic susceptibility versus inverse of  $N$  sites for an itinerant electron density of  $x = 0.2$  and  $JS^2/t = 0.2$ . Solid circles, cross, plus and open circles represent four different temperatures  $k_B T/t = 0.1, 1, 2$  and  $3$ , respectively. Fitting solid lines are also shown in the same figure.

former lines. At high temperature Curie–Weiss behavior was obtained. As shown, Curie constant is basically  $t$ – $J$  independent. Our Ising-like results give  $C = 1 + 3x$  or  $C = 4 - 3n$ . Kojima *et al.* from experimental results proposed  $C \simeq 3n$  ( $S = 1/2$ ). In our case we remove electrons from an  $S = 1$  system  $n = 0$ . In the case of Kojima, holes are added. In this case our Ising-like model may be related with experimental results. Curie–Weiss temperature  $T_c$  is  $t$ – $J$  dependent and can be related with Curie-like behavior observed in this compound.<sup>21,22</sup> It is important to mention that the contribution related to the Haldane gap in  $S = 1$  spin chains decreases exponentially with decreasing temperature and becomes negligible at low temperature  $T < 20$  K.<sup>28</sup> It is difficult to identify the different contributions to the magnetic susceptibility in such a complex magnetic ground state. Of course, our comparison with the experimental results becomes irrelevant below the spin-glass transition identified to be  $T_g \sim 2.9$  K. Finite size effects are taken into account to show that our  $N = 20$  sites are of relevance. Inverse of magnetic susceptibility vs inverse of  $N$  sites for different temperatures are shown in Figs. 11 and 12 for an itinerant electron density of  $x = 0.2$  and  $x = 0.25$ , respectively. Fitting solid lines  $\alpha + \beta(1/N)$  with an error of  $10^{-4}$ , 95% of confidence levels are shown in the same figures. As can be seen in the same figures an error of  $\beta(1/N) \sim 10^{-2}$  is obtained if  $N = 20$  sites are taken into account. The  $t = J = 0$  limit, that is  $N$ -site independent, is also compared with these thermodynamic limits, giving an error of  $10^{-1}$ .<sup>a</sup> Finite size effects for a Heisenberg and an Ising model (without itinerant electrons  $x = 0$ ) were studied in Refs. 26 and 27. As can be seen in those references,

<sup>a</sup>It is important to mention that another itinerant electronic densities and SE couplings were considered. Almost the same errors were obtained and the same qualitative behavior in magnetic susceptibility and spin–spin correlations.

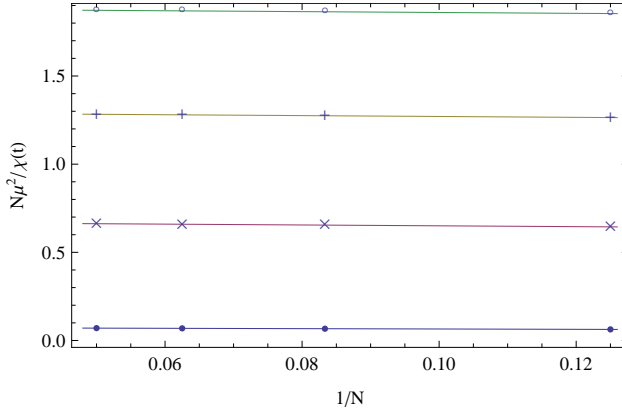


Fig. 12. The same as Fig. 11 but for an itinerant electron density of  $x = 0.25$ .

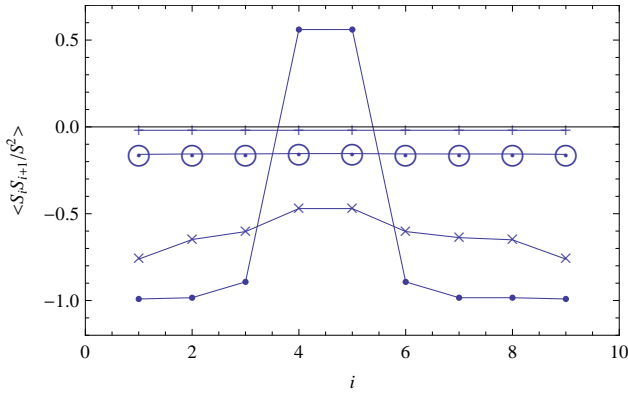


Fig. 13. The same as Fig. 6 but for a chain of  $N = 10$  sites, one itinerant electron  $x = 0.10$  is presented.

magnetic susceptibility is almost  $N$ -site independent at high temperature limit. In our model, because of itinerant electrons, both high and low temperature limits lead to the same qualitative behavior.

It is also presented, in Fig. 13, short-range spin-spin correlations for one itinerant electron and  $N = 10$  sites,  $x = 0.1$  and  $JS^2/t = 0.2$ . These results can be compared with results shown in Fig. 6 for  $N = 20$  sites and two itinerant electrons. The same spin-spin correlations behavior can be observed. Magnetic phase diagram for classical localized spins and an exchange model, as used in this paper, is compared with the thermodynamic limit in Ref. 16. As can be observed in that reference, the same magnetic phases were obtained.

Of course that because of our exact results very long systems cannot be studied easily because of a huge CPU time used.

## 4. Conclusion

In this work, we presented exact parallel static magnetic susceptibility calculations and short-range spin–spin correlations of an equivalent Ising-like DE+SE model using large Hund’s coupling. Magnetic susceptibility was calculated in a region where P3–AF and F–AF phase separation can be found. At high temperature Curie–Weiss behavior and a very low correlated system were obtained. Curie constant is basically  $t - J$  independent and could be related with the Curie-like behavior observed in the nickelate one-dimensional compound  $Y_{2-n}Ca_nBaNiO_5$ . Finite size effects were considered to show the relevance of our finite  $N = 20$  system.

## Acknowledgment

We want to acknowledge partial support from CONACyT Grant-57929 and PAPIIT-IN108907 from UNAM. EV wants to acknowledge Dr. Calderon for using the cluster.

## References

1. C. Zener, *Phys. Rev.* **82**, 403 (1951).
2. C. Zener, *Phys. Rev.* **81**, 440 (1951).
3. P. W. Anderson and H. Hasegawa, *Phys. Rev.* **100**, 675 (1955).
4. P. G. de Gennes, *Phys. Rev.* **118**, 141 (1960).
5. S. Yunoki *et al.*, *Phys. Rev. Lett.* **80**, 845 (1998).
6. E. Dagotto *et al.*, *Phys. Rev. B* **58**, 6414 (1998).
7. S. Yunoki and A. Moreo, *Phys. Rev. B* **58**, 6403 (1998).
8. M. Yamanaka, W. Koshibae and S. Maekawa, *Phys. Rev. Lett.* **81**, 5604 (1998).
9. C. D. Batista *et al.*, *Phys. Rev. B* **58**, R14689 (1998).
10. C. D. Batista *et al.*, *Phys. Rev. B* **62**, 15047 (2000).
11. W. Koshibae *et al.*, *Phys. Rev. Lett.* **82**, 2119 (1999).
12. D. J. Garcia *et al.*, *Phys. Rev. Lett.* **85**, 3720 (2000).
13. D. J. Garcia *et al.*, *Phys. Rev. B* **65**, 134444 (2002).
14. H. Aliaga *et al.*, *Phys. Rev. B* **64**, 024422 (2001).
15. D. R. Neuber *et al.*, *Phys. Rev. B* **73**, 014401 (2006).
16. E. Vallejo *et al.*, *Solid State Commun.* **149**, 126 (2009).
17. J. R. Suárez *et al.*, *J. Phys.: Condens. Matter* **21**, 046001 (2009).
18. D. C. Mattis, *The Theory of Magnetism Made Simple* (World Scientific, 2006).
19. G. H. Jonker and J. H. Van Santen, *Physica* **16**, 337 (1950).
20. J. H. Van Santen and G. H. Jonker, *Physica* **16**, 599 (1950).
21. K. Kojima *et al.*, *Phys. Rev. Lett.* **74**, 3471 (1995).
22. J. F. DiTusa *et al.*, *Phys. Rev. Lett.* **73**, 1857 (1994).
23. E. Vallejo and M. Avignon, *Phys. Rev. Lett.* **97**, 217203 (2006).
24. L. F. Mattheiss, *Phys. Rev. B* **48**, 4352 (1993).
25. K. Penc and H. Shiba, *Phys. Rev. B* **52**, R715 (1995).
26. J. C. Bonner and M. E. Fisher, *Phys. Rev.* **135**, A640 (1964).
27. M. E. Fisher, *Am. J. Phys.* **32**, 343 (1964).
28. J. Das *et al.*, *Phys. Rev. B* **69**, 144404 (2004).